

rates for irradiation energies from 0.15 to 2.1 MeV has been performed by Iseler *et al.*<sup>2</sup> The analysis of those data dealt with the entire energy range so that the features of multiple-atomic-defect production were emphasized. This paper shows that for irradiation energies less than 0.20 MeV the theoretical and experimental damage rates have the best agreement when the probability of atomic displacement is a multiple step function (see curve a of Fig. 2). Uncertainties are present in the analysis because the magnitudes of the corrections are of the order of the experimental values. It is shown that each correction introduces an effect that prevents a well-defined intersection between the damage-rate curve and the abscissa. It is evident from these results that high-purity aluminum does not have an appreciable amount of subthreshold damage.

It is generally accepted<sup>14</sup> that the electron irradiation of a metal produces simple point defects of interstitials and vacancies. Defects which recover during stage I are

<sup>14</sup> J. W. Corbett, in *Solid State Physics*, edited by F. Seitz and D. Turnbull (Academic Press Inc., New York, 1966).

caused by the annihilation of interstitials which are either bound to vacancies (these reactions obey first-order kinetics) or migrate through the lattice (diffusion-limited reaction). Trapping is a mechanism which prevents the complete recombination of interstitials and vacancies during stage I. Because trapping is a process that depends on the distance that an interstitial is separated from its initial lattice site, one deduces that the fraction of the damage which does not anneal during stage I should increase monotonically with the irradiation energy.<sup>9</sup> In order to obtain the desired energy dependence for the stage-I recovery of aluminum, the total induced damage has been resolved into subthreshold and intrinsic components, and the subthreshold damage is assumed to be independent of the irradiation energy. The calculations based on these assumptions give results which account for the observed energy dependence of stage I for aluminum. This interpretation of the data is consistent with the known facts that the amount of subthreshold damage is appreciable for copper<sup>13</sup> but small for aluminum.<sup>1</sup>

## Coherent Neutron Scattering by Cobalt with Nuclear Polarization\*

Y. ITO† AND C. G. SHULL

*Massachusetts Institute of Technology, Cambridge, Massachusetts 02139*

(Received 10 March 1969)

The polarized-neutron diffraction technique has been used to determine the modification of coherent scattering with nuclear polarization in cobalt. This was studied in two Bragg reflections, (220) and (140), from a crystal of hexagonal cobalt at temperatures as low as 2.23°K, with nuclear polarization being developed by hyperfine field interaction in the ferromagnetic element. From these observations, the spin-state scattering amplitudes  $b_+$  and  $b_-$ , corresponding to neutron-nucleus compound states of spin  $I+\frac{1}{2}$  and  $I-\frac{1}{2}$ , respectively, have been determined as  $(-0.380 \pm 0.054) \times 10^{-12}$  and  $(+1.060 \pm 0.070) \times 10^{-12}$  cm. These values are found to be consistent with the coherent scattering amplitude as obtained in unpolarized-neutron-unpolarized-nucleus studies, and with the known neutron resonance level structure in cobalt.

### I. INTRODUCTION

THE scattering of thermal neutrons by nuclei of spin  $I$  is described in terms of the two spin-state amplitudes  $b_+$  and  $b_-$ , which are associated with the total spin states  $I+\frac{1}{2}$  and  $I-\frac{1}{2}$  of the compound neutron-nucleus system, respectively. These spin-dependent scattering amplitudes provide useful information relative to the energy levels of the compound nucleus in the vicinity of thermal energy, and in a practical sense knowledge of them is significant, since they determine the coherent and incoherent scattering to be found by an assembly of nuclei in a crystal.

If the scattering nuclei are unpolarized, as is usually the case at normal temperature, it is convenient to introduce combinations of the spin-state amplitudes into the coherent and incoherent scattering amplitudes  $b_c$  and  $b_i$  as follows:

$$b_c = \frac{I+1}{2I+1} b_+ + \frac{I}{2I+1} b_-, \quad (1)$$

$$b_i = \frac{2}{2I+1} (b_+ - b_-). \quad (2)$$

These quantities are used extensively in neutron-diffraction investigations, since they describe the nuclear-scattering contribution to the coherent Bragg intensity and the incoherent, spin disorder scattering from a crystal. Values for  $b_c$ , both in magnitude and absolute sign, have been determined by experiment for

\* Research supported by the Division of Research, U. S. Atomic Energy Commission. It is based on a thesis submitted by the senior author to the Department of Physics at the Massachusetts Institute of Technology in partial fulfillment of the requirements for the degree of Doctor of Philosophy.

† Present address: Ames Laboratory, Iowa State University, Ames, Iowa 50010.

many nuclei in crystal scattering or by mirror reflection. Likewise, an experimental study of the spin disorder scattering can yield the magnitude of  $b_i$  but not its sign, because scattering-phase information is lacking in incoherent scattering. Thus it is not possible to assign unique values to the spin-state scattering amplitudes from scattering data obtained with unpolarized nuclei.

On the other hand, if scattering of polarized neutrons by polarized target nuclei is realized,<sup>1,2</sup> the spin weighting factors of Eqs. (1) and (2) are modified in a known fashion, and a unique determination of  $b_+$  and  $b_-$  becomes possible. In this way, Shull and Ferrier<sup>3</sup> succeeded in observing an increase in coherent Bragg scattering of polarized neutrons from vanadium due to nuclear polarization, and this permitted unambiguous assignment to the spin scattering amplitudes. They employed the "brute-force" method of attaining nuclear polarization through action of an externally applied magnetic field at temperatures as low as 2.8°K.

In the present work, the spin-state amplitudes for cobalt (or Co<sup>59</sup> since the element is isotopically pure) have been determined in a similar way except that the polarizing field is now much enhanced over the applied field by the hyperfine interaction.<sup>4</sup> The experiments have been carried out with single crystals of the ferromagnetic element within which the polarizing field, and hence the degree of nuclear polarization, is magnified some 15 times over that of the applied field. The modification in  $b_c$  with nuclear polarization was studied with polarized neutrons in two Bragg reflections, (220) and (140) for which the magnetic scattering amplitudes arising from the ferromagnetic structure are of opposite sign. The ferromagnetic scattering by hexagonal cobalt has been thoroughly studied at room temperature by Moon<sup>5</sup> and, because of the high Curie temperature, very little change occurs in the magnetic scattering on reducing the temperature into the nuclear polarization region. An earlier study by Schermer<sup>6</sup> has studied the change in the total scattering and absorption cross section of cobalt with nuclear polarization from measurements on the transmission of polarized neutrons through a polycrystalline sample. The present work complements the Schermer experiment in being carried out at higher temperatures than with Schermer's adiabatic demagnetization temperatures and with sensitivity to effects arising only from scattering.

## II. GENERAL SCATTERING CROSS SECTIONS WITH NUCLEAR POLARIZATION

Cross-section formulas for the coherent scattering of polarized thermal neutrons from polarized target nuclei

<sup>1</sup> M. E. Rose, U. S. Atomic Energy Commission Document No. AECD-2183, 1948 (unpublished).

<sup>2</sup> C. G. Shull and E. O. Wollan, Phys. Rev. **81**, 527 (1951).

<sup>3</sup> C. G. Shull and R. P. Ferrier, Phys. Rev. Letters **10**, 295 (1963).

<sup>4</sup> C. J. Gorter, Physica **14**, 504 (1948); M. E. Rose, Phys. Rev. **75**, 213 (1949).

<sup>5</sup> R. M. Moon, Phys. Rev. **136**, A195 (1964).

<sup>6</sup> R. I. Schermer, Phys. Rev. **130**, 1907 (1963).

were first derived by Rose<sup>1</sup> for the simplest case of purely nuclear scattering. This was extended by Schermer<sup>6</sup> to the case where magnetic scattering from a uniaxial magnetic substance is encountered and by Schermer and Blume<sup>7</sup> to cases of arbitrary spin ordering with additional treatment of the change in neutron polarization upon scattering.

For the case of a monoisotopic and uniaxial magnetic material (such as cobalt under present observation) the total coherent scattering amplitude  $B_c$  arising from magnetic scattering combined with modified nuclear scattering becomes

$$B_c = b_c \pm \delta \pm p, \quad (3)$$

with

$$\delta = \frac{1}{2} b_i I f_N, \quad (4)$$

where  $f_N$  is the nuclear polarization, and  $p$  is the magnetic scattering amplitude. The upper pair of signs correspond to neutron polarization parallel to the nuclear polarization (or electronic polarization), whereas the lower pair of signs is representative of the antiparallel case. Since  $p$  depends upon the scattering angle through the magnetic form factor, whereas  $b_c$  and  $b_i$  are isotropic, the total coherent scattering amplitude  $B_c$  is angle-dependent. Moreover,  $B_c$  will depend upon temperature through both the  $\delta$  and  $p$  terms.

The nuclear polarization can be described as

$$f_N = \text{tr}\{\rho I_z\} / I \text{tr} \rho \quad (5)$$

in terms of the density matrix  $\rho$  of the nuclear spin system. Using the Boltzmann form for the density matrix, this becomes

$$f_N = B_I(g_N \beta_N H_{\text{eff}} / kT), \quad (6)$$

where  $B_I(y)$  is the Brillouin function,  $g_N$  is the nuclear  $g$  factor,  $\beta_N$  is the nuclear Bohr magneton, and  $H_{\text{eff}}$  is the effective magnetic field acting at the nuclear site. For small values of  $f_N$  (in the present experiment this was at most  $7 \times 10^{-3}$ ), this can be closely approximated as

$$f_N = \frac{1}{3} [I(I+1) / (kT)] g_N \beta_N H_{\text{eff}} \quad (7)$$

and

$$\delta = \frac{1}{6} [I(I+1) / kT] b_i g_N \beta_N H_{\text{eff}}. \quad (8)$$

Since the variation of  $p$  with temperature is well known from saturation magnetization-versus-temperature experiments, the magnitude and sign of  $b_i$  may be determined from the temperature variation of  $B_c$  provided other terms in Eq. (8) are known. In particular, a knowledge of  $H_{\text{eff}}$ , containing components of the applied field, hyperfine field, and demagnetization field, is required as discussed in Sec. IV G.

The experimental study of  $B_c$  is accomplished through measurement of the intensity in Bragg reflections as a function of neutron polarization and temperature. The Bragg intensity will be proportional to the coherent differential scattering cross section  $\sigma(\theta)$ ; with arbitrary neutron polarization  $f_n$ , this can

<sup>7</sup> R. I. Schermer and M. Blume, Phys. Rev. **166**, 554 (1968).

be expressed as

$$\sigma(\theta) = (b_c^2 + 2f_n b_c \delta + \delta^2) + 2(f_n b_c + \delta)p + p^2. \quad (9)$$

With perfect neutron polarization  $f_n = \pm 1$ ; this is recognized as the square of  $B_c$  given by Eq. (3).

The quantity of interest for the interpretation of experimental data is the polarization ratio  $R$ , defined as the intensity ratio upon reversal of the neutron polarization direction with respect to the atomic magnetization or nuclear polarization directions. This becomes

$$R = \frac{\sigma_+(\theta)}{\sigma_-(\theta)} = \frac{b_c^2 + 2b_c \delta |f_n| + \delta^2 + 2(b_c |f_n| + \delta)p + p^2}{b_c^2 - 2b_c \delta |f_n| + \delta^2 - 2(b_c |f_n| - \delta)p + p^2}. \quad (10)$$

An ideal experiment would have  $|f_n| = 1$ , for which the polarization ratio becomes

$$R_0 = \left( \frac{b_c + \delta + p}{b_c - \delta - p} \right)^2 = \left( \frac{1 + \alpha + \beta}{1 - \alpha - \beta} \right)^2, \quad (11)$$

with  $\alpha = p/b_c$  and  $\beta = \delta/b_c$ . It will be convenient to rearrange Eq. (11) into

$$\alpha + \beta = \frac{\sqrt{R_0} \mp 1}{\sqrt{R_0} \pm 1}, \quad (12)$$

with the upper set of signs corresponding to  $|\alpha + \beta| < 1$  and the lower set to  $|\alpha + \beta| > 1$ . All of the present experimental data correspond to  $|\alpha + \beta| < 1$ .

The parameter  $\beta$  will depend upon the nuclear polarization through Eq. (8) and hence will depend strongly upon the temperature. On the other hand,  $\alpha$  will remain essentially constant for the temperature range covered by the present experiment because of the very high Curie temperature for cobalt.

### III. EXPERIMENTAL PROCEDURES

In order to study the nuclear polarization effect on the coherent scattering amplitude, polarization-ratio measurements have been made at various temperatures as low as 2.23°K for two Bragg reflections, (220) and (140), from a single crystal of ferromagnetic, hexagonal cobalt. Cobalt was selected for study because it was known to possess a favorable amplitude ratio  $b_i/b_c$  and also to exhibit a large hyperfine field. Both factors are significant in obtaining measurable effects at modestly low temperature attainable by pumping liquid helium.

The two reflections (220) and (140) were selected for the following reasons:

(a) The strong magnetic anisotropy of hexagonal cobalt necessitates the use of reflections of the type ( $hk0$ ) in order to realize full magnetic saturation with an applied field of reasonable strength. Our experi-

mental conditions required a vertical field and horizontal plane of scattering.

(b) A small value of the magnetic scattering amplitude  $p$  is desirable in order to distinguish clearly  $\beta$  and  $\alpha$  in Eq. (12). Since the value of  $p$  or  $\alpha$  is strongly dependent upon  $(\sin\theta)/\lambda$  and in fact reverses its sign as Moon has shown<sup>6</sup> at sufficiently large angles, reflections near this crossover region will be expected to show minimum competition of magnetic scattering with the nuclear polarization scattering.

(c) Various corrections to the experimental measurements must be made as will be discussed in Sec. IV, and the use of high index reflections generally lessens the size of these corrections. Moreover, since  $p$  or  $\alpha$  is positive for the (220) reflection and negative for the (140) reflection, the corrections enter in a different manner with different magnitude for the two reflections. Confidence in the validity of the corrections is gained from agreement in the results for the two reflections.

The crystal specimen that was used in the experiment was cut and surfaced into approximately ellipsoidal shape with axes 9.5, 4.8, and 2.4 mm oriented with the hexagonal  $c$  axis in the long direction. It was mounted inside a helium-flow cryostat, where its temperature was controlled by a surrounding bath of either liquid helium or helium vapor. This cryostat system was designed for use in a vertical field, iron-core electromagnet capable of producing 15-kG field with a pole separation of 2.54 cm. The magnet-cryostat system was mounted on a goniometer at the second axis of a double axis, polarized-beam spectrometer in which a polarized, monochromatic beam of slow neutrons is prepared at the first axis by a conventional Co-Fe polarizing crystal. All magnetic fields and the neutron polarization are in the vertical direction with the plane of scattering being horizontal. In passage from the first axis to the second axis, the neutron polarization could be inverted with high efficiency from the normally up orientation by rf excited resonance transition, thereby permitting a determination of the polarization ratio defined earlier. The specimen crystal was mounted in the cryostat-magnet system with its  $c$  axis vertical, i.e., parallel to the magnetic field and coaxial with the neutron polarization. Temperatures could be controlled ( $\pm 0.02^\circ\text{K}$  at  $2.23^\circ\text{K}$ ) by feedback arrangement on the helium-flow system and were determined with a calibrated carbon resistor.

Although the incident neutron polarization was very high, 0.996 and 0.990 for normal and inverted polarized beams, respectively, a noticeable depolarization (with a temperature dependence) was found to occur in the passage of the beam through the crystal specimen.

The depolarization factor changes from 0.990 at room temperature to 0.980 below  $30^\circ\text{K}$ . This was studied by placing a polarization-analyzing crystal behind the specimen crystal, thereby sensing the polarization in the transmitted beam. Such depolar-

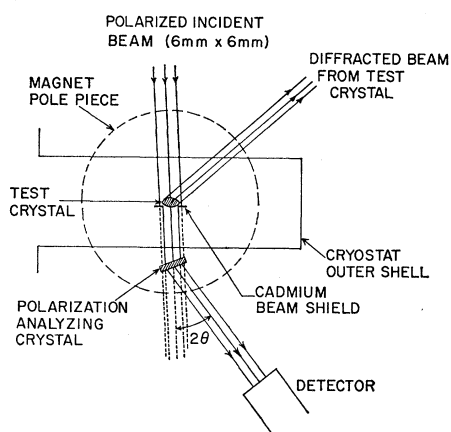


Fig. 1. Diagram of experimental assembly permitting measurement of polarization ratio in Bragg-reflected beam and depolarization of neutron beam within crystal specimen.

ization could arise from the action of (a) a nonuniform fringe field outside the specimen crystal, (b) a mistipping of the crystal  $c$  axis from the applied field direction, or (c) by incomplete magnetic saturation within the crystal specimen. Detailed studies showed that the fringe field inhomogeneity was the principal offender, and it was decided to arrange the system so that both the polarization ratio measurements and the beam depolarization could be measured under exactly the same conditions without changing the crystal orientation in the incident beam. The experimental arrangement for accomplishing this is shown schematically in Fig. 1, where the two measurements could be made by merely changing the neutron detector position without disturbing the crystal orientation or temperature. The specimen crystal was placed at the center of rotation of the detector. The noncentral position of the polarization-analyzing crystal caused a small angular deviation of the diffracting beam from this crystal. This was properly taken into account by the corresponding adjustment of the detector  $2\theta$  position and also by the relatively wide counter window.

In studying the two Bragg reflections, it was necessary to change the neutron wavelength from 1.050 Å used for the (220) reflection to 0.796 Å for the (140) reflection because of scattering-angle limitations on the spectrometer and in the cryostat. Although the use of a reduced wavelength resulted in a lesser reflection intensity and correspondingly a larger statistical error in the data results, this was compensated somewhat by having smaller corrections to be applied to the measured data. Polarization-ratio measurements and beam-depolarization studies were carried out for both reflections at temperatures of 293, 30, 4.22, and 2.23°K.

#### IV. CORRECTIONS TO THE EXPERIMENTAL DATA

Because of nonideal experimental conditions, various factors must be allowed for in applying Eq. (12) to

the analysis of the experimental data. These arise primarily from two sources: (a) imperfect neutron polarization within the crystal and (b) the presence of secondary extinction in the Bragg reflection process, although additional effects which are on a scale not requiring correction in the present experiment are worthy of discussion.

#### A. Neutron Polarization

It was mentioned above that the neutron beam polarization is modified in passing into the crystal and that emphasis must be placed on the determination of the effective neutron polarization to be associated with the crystal scattering. It can be shown that the mean value for the neutron polarization  $P$  within the crystal is related to the unperturbed incident polarization  $P_0$  as

$$P = P_0(P_T/P_0)^{1/2}, \quad (13)$$

where  $P_T$  is the transmitted beam polarization as measured in the scheme of Fig. 1. In the assessment of either  $P_0$  or  $P_T$ , allowance must be made for incomplete efficiency in the polarization inversion and for the higher-order  $\frac{1}{2}\lambda$  wavelength component (with different polarization) in the incident beam. All of these factors are measurable, and detailed analysis shows that the measured polarization ratio of a Bragg reflection beam  $R_m$  can be corrected for all of these effects in a straightforward manner to become  $R'$ .

#### B. Secondary Extinction

The presence of secondary extinction in the crystal specimen implies that the measured Bragg intensity is not directly proportional to the scattering cross section and that a measured polarization ratio is not given by the ratio of two scattering cross sections as exhibited in Eq. (10). This effect is usually minimized by reducing the crystal thickness or distorting the crystal, thereby increasing the mosaic width. Neither procedure was practical for the case of these high-angle reflections because of the sizable intensity loss that would be experienced. In spite of the fact that extinction effects are reduced with high index reflections, there are troublesome features associated with the relatively high absorption of the neutron beam in cobalt, with the unsymmetrical reflection arrangement employed in the experiment, and with the changes at low temperature; these offer difficulties in applying the necessary corrections. In view of this, three independent procedures were used for assessing the extinction, and their intercomparison gave information on the validity of the extinction correction.

The first procedure involved the direct experimental determination of the mosaic-width parameter by performing a double-crystal rocking experiment with the test crystal being bathed in radiation from a matched-spacing, perfect crystal. This gives an upper limit to the mosaic width and hence a limit to the degree of

extinction. Secondly, if we accept Moon's values for the polarization ratios at room temperature<sup>8</sup> as being extinction-corrected, a comparison with the polarization ratios measured with the present crystal can lead to the extinction correction within limits. Finally, the present experiment covers a wide temperature range over which the scattering cross section should vary with nuclear polarization in a known way, namely, with the  $T^{-1}$  Curie-law dependence, and one can estimate the extinction from the temperature dependence as determined experimentally.

The three approaches were found to be reasonably consistent with each other in terms of predicting the true extinction correction. Accordingly, they have been combined together, and the uncertainty in the final extinction correction was taken from the range displayed by the separate methods. The uncertainty of the extinction correction is rather larger than that associated with the beam polarization and contributes about 35% to the final probable error of the results.

### C. Crystal Effects

Several other effects which are related to the physical state or orientation of the single-crystal specimen are worthy of mention. The first is that arising from the presence of simultaneous reflections in which the observed intensity from the primary reflection has superimposed intensity from a composite pair of Bragg reflections within the crystal. This was studied by rotating the crystal around the scattering-vector axis, thereby changing simultaneous-reflection effects but not that of the primary reflection, and no intensity disturbance was measurable. Thus the perturbation arising from simultaneous-reflection conditions must have been either unmeasurably small or else were self-canceling.

With measurements being performed over the temperature range from room temperature to 2.23°K, effects arising from the thermal contraction of the lattice, the change in Debye-Waller factor, the small variation of the magnetic scattering amplitude, and changes in the magnetic anisotropy of the crystal must be investigated. These have all been considered and either incorporated into the above correction scheme or shown to be negligible.

The purity of the single-crystal specimen was stated to be 99.95%, with major impurities Fe(0.04%) and Ni(0.02%), and no corrections were called for relative to the precision of the results. Cobalt is known to crystallize in both hexagonal and fcc form and stacking faults, in which both phases are mixed, are known to occur frequently. The presence of fcc regions in our specimen crystal would be troublesome because the hyperfine field, and hence the degree of nuclear polarization, is known to differ somewhat in the two phases.<sup>8</sup>

<sup>8</sup> Y. Koi, A. Tsujimura, and T. Kushida, *J. Phys. Soc. Japan* **15**, 2100 (1960).

We have searched for the presence of intensity at fcc reflection positions with the present specimen crystal, and, not finding any, we conclude that it is very dominant in the hexagonal phase.

### D. Temperature Variation of Nuclear Capture Cross Section

When both neutrons and nuclei are polarized, the capture cross section becomes spin-dependent,<sup>1</sup> just as in the scattering case, and can be expressed as

$$\sigma_a = \sigma_{0a} + f_n f_N \sigma_{pa},$$

with  $\sigma_{0a}$  being the usual absorption cross section (unpolarized nuclei) and the polarization-dependent part given by

$$\sigma_{pa} = [I/(2I+1)](\sigma_a^+ - \sigma_a^-),$$

with  $\sigma_a^+$  and  $\sigma_a^-$  being the spin-state absorption cross sections. Schermer<sup>6</sup> has studied the quantity  $\sigma_{pa}$  and using his results we have calculated the effect of a changing cross section on our scattering results and find them negligibly small.

### E. Other Scattering Interactions

In addition to the nuclear and magnetic scattering interaction treated above, neutrons can interact with atoms through the specific neutron-electron interaction<sup>9</sup> and through the neutron-orbit-Coulombic-field interaction.<sup>10</sup> The strengths of these effects are known, and we have investigated their perturbation on the present results and again find them to be negligible within the precision of the results.

### F. Inelastic Scattering Effects

In measuring the polarization ratio at the Bragg-reflection position, it is necessary to consider whether inelastic scattering effects, and their neutron polarization dependence, are perturbing the results beyond that characteristic of pure elastic scattering. This inelastic scattering can arise from interaction of the neutron with lattice phonons (referred to as magnetovibrational scattering in the case of coexistent magnetic and nuclear structure) or with the magnetic spin structure itself (through creation or annihilation of spin waves or magnons). It can be shown that the magnetovibrational scattering intensity will possess the same dependence on the nuclear and magnetic scattering amplitudes and the neutron polarization as is seen in the elastic Bragg scattering for the case where the magnetization is directed perpendicular to the scattering vector. This is characteristic of the present experiment, and hence the expression for the polarization ratio  $R$ , Eq. (10), is still valid even when the intensity contains a magnetovibrational component.

<sup>9</sup> V. E. Krohn and G. R. Ringo, *Phys. Rev.* **148**, 1303 (1966).

<sup>10</sup> C. G. Shull, *Phys. Rev. Letters* **10**, 297 (1963).

On the other hand, the magnon scattering is independent of neutron polarization as Saenz<sup>11</sup> has shown, and Eq. (10) will be inexact in describing the polarization ratio if there is a measurable magnon intensity at the Bragg-reflection center over and above that included outside the Bragg reflection which supplied a background correction. However, the magnon scattering cross section depends upon the square of the magnetic form factor, and this factor is very small for these outer-angle reflections. This, coupled with the fact that the measurements are performed at low temperatures, would imply a negligible magnon-intensity contribution. Actually, when nuclear polarization effects are included, nuclear spin waves will accompany electronic spin waves by the hyperfine field interaction and the "magnon" cross section<sup>12</sup> should include a dependence upon  $\delta$ . This again is expected to be negligibly small under the present conditions.

### G. Effective Polarizing Field at Nuclear Site

In assessing the nuclear polarization  $f_N$  with Eq. (7), it is necessary to evaluate the various contributions to the polarizing field  $H_{\text{eff}}$ . This can be expressed as

$$\begin{aligned} H_{\text{eff}} &= H_{\text{hfs}} + H_0 + \frac{4}{3}\pi M_s - DM_s \\ &= H_{\text{hfs}} + H_{\text{loc}}, \end{aligned} \quad (14)$$

where  $H_{\text{hfs}}$  is the hyperfine field at the nuclear position arising from the atomic magnetization,  $H_0$  is the externally applied field,  $\frac{4}{3}\pi M_s$  is the Lorentz field, and  $DM_s$  is the demagnetizing field dependent upon sample geometry. Throughout the experimentation, the applied field  $H_0$  was kept at 14.75 kOe,  $D$  was evaluated as 1.50 from the crystal dimensions, and with the saturation magnetization<sup>13</sup>  $M_s = 1446$  Oe,  $H_{\text{loc}}$  is evaluated as  $18.5 \pm 0.5$  kOe, with the uncertainty arising from the demagnetizing factor. For the hyperfine field, we use the NMR data of Koi *et al.*,<sup>8</sup> who measured zero-field resonance at  $228.0 \pm 0.5$  Mc/sec for hexagonal cobalt. With the cobalt nuclear magnetic moment of  $4.639 \mu_N$ ,  $H_{\text{hfs}}$  is evaluated as  $225.7 \pm 0.5$  kOe. The sign of the hyperfine field has been determined to be negative from the Mössbauer study of Dash *et al.*,<sup>14</sup> i.e., opposite

<sup>11</sup> A. W. Saenz, Phys. Rev. **119**, 1542 (1960).

<sup>12</sup> This suggests the interesting possibility of observing nuclear spin waves as generated by magnons under conditions where the magnons are not visible in neutron scattering. Because of the dependence of scattering cross section (see Ref. 11) upon the directions of neutron polarization, the scattering vector, and the magnetization, this could be done most effectively where all three directions are coincident, for which magnetic elastic and magneto-vibrational would be absent. Furthermore, a high-angle reciprocal lattice vector near the form-factor crossover would allow  $\delta \rightarrow 0$ , and hence the normal magnon scattering would become vanishingly small. For this case, the inelasticity realized in the nuclear spin-wave scattering is characteristic of the electronic spin states and not the nuclear spin states.

<sup>13</sup> R. M. Bozorth, *Ferromagnetism* (D. Van Nostrand, Inc., Princeton, N. J., 1951).

<sup>14</sup> J. G. Dash, R. D. Taylor, P. P. Craig, D. E. Nagle, D. R. F. Cochran, and W. E. Keller, Phys. Rev. Letters **5**, 152 (1960).

TABLE I. Summary of experimental results.<sup>a</sup>

(hkl)	Temp. (°K)	$R_m^b$	$R'^c$	$R^d$	$\alpha + \beta$
(220)	293	1.2027(18)	1.2063(27)	1.2200(40)	+0.0497(9)
	30	1.2022(15)	1.2079(24)	1.2279(32)	+0.0513(7)
	4.22	1.2354(18)	1.2422(26)	1.2673(34)	+0.0592(7)
	2.23	1.2666(17)	1.2745(26)	1.3050(35)	+0.0665(7)
(140)	293	0.9177(39)	0.9162(44)	0.9143(60)	-0.0224(16)
	30	0.9266(33)	0.9247(36)	0.9215(47)	-0.0204(13)
	4.22	0.9561(31)	0.9549(34)	0.9528(45)	-0.0121(12)
	2.23	0.9850(38)	0.9846(40)	0.9839(52)	-0.0040(13)

<sup>a</sup> Numbers in parentheses are standard errors.

<sup>b</sup>  $R_m$  is the measured polarization ratio.

<sup>c</sup>  $R'$  is the polarization ratio after correction for  $\lambda$ -order contaminant, incomplete incident neutron polarization, depolarization of neutron beam, and incomplete polarization inversion.

<sup>d</sup>  $R$  is the polarization ratio after additional correction for secondary extinction.

to the magnetization direction, and hence  $H_{\text{eff}}$  becomes  $-207.2$  kOe.

### V. EXPERIMENTAL RESULTS AND DISCUSSION

The experimentally determined polarization ratios for the two Bragg reflections at various temperatures are collected in Table I under the column heading  $R_m$ . These ratio values were first corrected for incomplete neutron polarization and higher-order wavelength effects to yield values listed as  $R'$ . Additional correction for secondary extinction effects was then applied leading to the fully corrected values labeled  $R$  in the table. Finally, the quantity  $\alpha + \beta$  was calculated using Eq. (12) for each reflection-temperature entry. The standard errors in the entries arise from the statistical accuracy of the measured quantities combined with the assessed accuracy of the corrections that were incorporated.

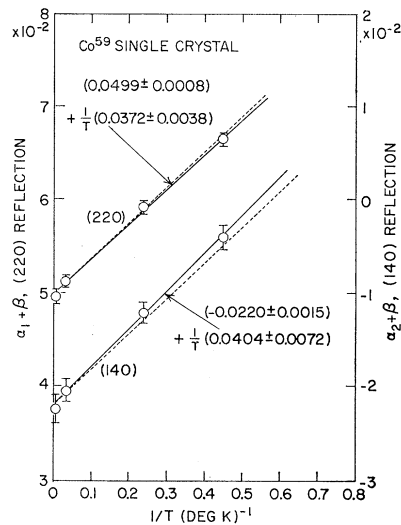


FIG. 2. Variation of nuclear polarization effect with temperature for two Bragg reflections showing Curie-law development of nuclear polarization. The solid lines represent least-squares fitting to the data and the dashed lines represent the best mean fitting to both sets of data.

Figure 2 displays the values of  $\alpha+\beta$  plotted against the inverse temperature for the separate reflection cases. The expected linear dependence of  $\alpha+\beta$  with  $T^{-1}$  is seen to be satisfied within the precision of the data. A least-squares fit to the data gives for the (220) reflection

$$\alpha_1+\beta = (+0.0499\pm 0.0008) + (0.0372\pm 0.0038)T^{-1},$$

and for the (140) reflection

$$\alpha_2+\beta = (-0.0220\pm 0.0015) + (0.0404\pm 0.0072)T^{-1},$$

where  $T$  is in  $^{\circ}\text{K}$ . The temperature-independent term of the above equations (the intercept of the straight line with the ordinate axis) immediately gives the magnetic scattering contribution  $\alpha$  separated from  $\beta$ , and this can be compared with the results obtained previously by Moon.<sup>5</sup> His results, when expressed as  $\alpha$  values, are

$$\alpha_1 = +0.0519\pm 0.0015$$

and

$$\alpha_2 = -0.0194\pm 0.0014,$$

both agreeing within experimental error with the present values. The reversed sign for  $\alpha$  at the two reflection positions corresponds to the inverted magnetic scattering amplitude as discussed earlier.

The effects of nuclear polarization are found in the  $\beta$  term (the slope of the temperature-dependence plot of Fig. 2), and it is seen that the two slope values are the same within experimental error. This is to be expected since the nuclear polarization  $f_N$  which is being sensed in the experiment is the component directed along the  $c$  axis for either reflection. In both cases the applied field is in the same direction with the same magnitude and hence  $H_{\text{eff}}$ , the total polarizing field, is the same. The mean value  $\Delta$  for the slope is obtained as  $+0.0379\pm 0.0033^{\circ}\text{K}$ , and hence from Eq. (8)

$$\Delta = \frac{1}{6}(b_i/b_c)(I+1)(\mu/k)H_{\text{eff}}.$$

Using the values  $b_c = +0.250\times 10^{-12}$  cm/atom (Moon<sup>5</sup>),  $\mu = 4.639 \mu_N$ , and  $H_{\text{eff}} = -207.2$  kOe, we obtain

$$b_i = (-0.360\pm 0.031)\times 10^{-12} \text{ cm/atom}.$$

When this is combined with  $b_c$ , the spin-state scattering amplitudes are evaluated as

$$b_+ = (-0.380\pm 0.054)\times 10^{-12} \text{ cm/atom},$$

$$b_- = (+1.060\pm 0.070)\times 10^{-12} \text{ cm/atom}.$$

These values may be compared with the alternative sets of values for  $b_+$  and  $b_-$ , which can be calculated from unpolarized beam studies of  $b_c$  and the total scattering cross section of  $6.7\pm 0.3$  b as measured by Wu, Rainwater, and Havens.<sup>15</sup> This yields the sets (all

<sup>15</sup> C. S. Wu, L. J. Rainwater, and W. W. Havens, Jr., *Phys. Rev.* **71**, 174 (1947).

in  $10^{-12}$  cm/atom)

$$b_+ = +0.85\pm 0.02, \quad b_- = -0.53\pm 0.03 \text{ (set I),}$$

$$b_+ = -0.35\pm 0.02, \quad b_- = +1.03\pm 0.03 \text{ (set II).}$$

It is seen that the present polarized beam scattering data determines set II as being the correct assignment. This agrees with the assignment given by Schermer<sup>6</sup> from polarized-beam-transmission measurements. It may be mentioned that the use of a positive hyperfine field leads to inconsistency between the values of  $b_+$  and  $b_-$  determined from the present nuclear-polarization data and the above unpolarized-beam results. Hence the present results can be considered as an indirect confirmation of the negative sense of the hyperfine field.

The interpretation of the spin-state scattering amplitudes given above requires a detailed understanding of the compound system of neutron and nucleus. It is to be noted that the magnitudes of both  $b_+$  and  $b_-$  are considerably removed, either in magnitude or sign, from any reasonable value for the potential scattering amplitude  $r_0$  or nuclear radius, which for cobalt would be expected to have a value of about  $+0.55\times 10^{-12}$  cm. This suggests the perturbing effect of nearby resonances (at energies other than the slow neutron energies) and indeed from the signs of the spin-state scattering amplitudes, dominant  $J=I+\frac{1}{2}$  (angular momentum of compound nucleus) resonances are called for at higher neutron energy and  $(I-\frac{1}{2})$  resonant states are indicated for lesser (negative) energy. In agreement with this, it is known that an  $(I+\frac{1}{2})$  resonance occurs in Co at 130 eV with a neutron width of 5.1 eV.<sup>16</sup> Using standard resonance-scattering theory with these single-resonance characteristics,  $b_+$  is evaluated as  $-0.21\times 10^{-12}$  cm. This is smaller in magnitude than the experimental value and the agreement can be improved, as Schermer<sup>6</sup> has pointed out, by assuming that additional higher-energy resonances are of  $I+\frac{1}{2}$  type. On the other hand, to account for the  $b_-$  value being larger than  $r_0$  it is necessary to assume the presence of resonance levels at negative energy with  $J=I-\frac{1}{2}$ . These have not been resolved or identified as yet.<sup>17</sup>

#### ACKNOWLEDGMENTS

We wish to acknowledge helpful assistance and discussions during the course of the experiments by W. C. Phillips, F. A. Wedgwood, H. Mook, R. Maglic, A. C. Nunes, C. S. Schneider, A. D'Addario, R. Mozzi, and N. C. Rasmussen.

<sup>16</sup> M. D. Goldberg *et al.*, in *Brookhaven National Laboratory Report No. 325* (U. S. Government Printing Office, Washington, D. C., 1966), 2nd ed., Suppl. 2, Vol. IIA.

<sup>17</sup> T. E. Stephenson, *Bull. Am. Phys. Soc.* **14**, 190 (1969). The two bound level parameters calculated by Stephenson indicate that the perturbing effect of the  $J=3$  level on the  $b_-$  is about 90% greater than that of the  $J=4$  level.